

# Synthesis, Crystal Chemistry, and Physical Properties of Ternary Intermetallic Compounds $An_2T_2X$ ( $An = Pu, Am$ ; $X = In, Sn$ ; $T = Co, Ir, Ni, Pd, Pt, Rh$ )

L. C. J. Pereira,\*<sup>†</sup> F. Wastin,\* J. M. Winand,\* B. Kanellakopoulos,<sup>‡</sup> J. Rebizant,\* J. C. Spirlet,\* and M. Almeida<sup>†,1</sup>

\*European Commission, Joint Research Centre, Institute for Transuranium Elements, Postfach 2340, D-76125 Karlsruhe, Germany;  
<sup>†</sup>Dept. Química, ITN, P-2686 Sacavém Codex, Portugal; and <sup>‡</sup>Forschungszentrum Karlsruhe, Institut für Technische Chemie, Postfach 3640, D-76125 Karlsruhe, Germany

Received January 24, 1997; in revised form July 16, 1997; accepted July 17, 1997

The synthesis, structural, and physical characterization of nine new ternary intermetallic compounds belonging to the isostructural  $An_2T_2X$  family with the transuranium Pu and Am elements, namely,  $Pu_2Ni_2In$ ,  $Pu_2Pd_2In$ ,  $Pu_2Pt_2In$ ,  $Pu_2Rh_2In$ ,  $Pu_2Ni_2Sn$ ,  $Pu_2Pd_2Sn$ ,  $Pu_2Pt_2Sn$ ,  $Am_2Ni_2Sn$ , and  $Am_2Pd_2Sn$ , are reported. From these compounds only  $Pu_2Rh_2In$ ,  $Am_2Ni_2Sn$ , and  $Am_2Pd_2Sn$  melt incongruently. All of these compounds crystallize in a tetragonal  $U_3Si_2$ -type structure, with the space group  $P4/mbm$ , ( $Z=2$ ) as most of the U and Np 2-2-1 compounds already found. In this structure,  $An$  atoms occupy the  $4h$  ( $x_1, x_1 + 0.5, 0.5$ ),  $T$  the  $4g$  ( $x_2, x_2 + 0.5, 0$ ), and  $X$  the  $2a$  ( $0, 0, 0$ ) positions. The average values of  $x_1$  and  $x_2$  are, respectively, 0.17 and 0.37. Single-crystal X-ray data were refined to  $R/R_w = 0.045/0.066, 0.043/0.072, 0.066/0.080, 0.070/0.098, 0.029/0.048, 0.055/0.080, 0.073/0.096, 0.048/0.086, 0.048/0.065$  for  $Pu_2Ni_2In, Pu_2Pd_2In, Pu_2Pt_2In, Pu_2Rh_2In, Pu_2Ni_2Sn, Pu_2Pd_2Sn, Pu_2Pt_2Sn, Am_2Ni_2Sn$ , and  $Am_2Pd_2Sn$ , respectively, for seven variables. The variation of the lattice parameters and the range of stability of the 2-2-1 phase are discussed in terms of the substitution of different  $An$  (actinide),  $T$  (transition metal), and  $X$  ( $p$ -electron) elements in their crystal structure. The possible role of spin fluctuations in the low-temperature behavior of the Pu samples is indicated by magnetic and electrical resistivity measurements.

© 1997 Academic Press

## INTRODUCTION

The systematic study of the physical properties of large families of intermetallic compounds sharing the same crystallographic structure is one of the most successful approaches in understanding the contribution of the  $f$  electrons in the bonding. Ternary intermetallics have provided such large isostructural families of compounds, where a

variety of different magnetic behaviors ranging from Pauli paramagnetism to heavy fermions, spin fluctuations or local-moment ferro- or antiferromagnetism could be found. In some of these compounds, in addition to their unusual magnetic behavior at very low temperatures, a transition to a superconducting state is also observed.

During the past few years intensive investigations have been devoted to a new isostructural family of ternary intermetallics,  $An_2T_2X$  ( $An =$  actinide element,  $T =$  transition element,  $X = p$ -element) (1–3). The study of the magnetic and electrical properties has revealed that the character of the  $5f$  states is strongly dependent on the strength of the  $5f-d$  hybridization, similar to what has been found in other actinide intermetallic compounds with transition metals (4–10). Especially in the case of the uranium series, the systematic occurrence of large linear specific heat coefficients at low temperatures,  $\gamma$ , indicative of heavy fermion behavior, in conjunction with the onset of antiferromagnetic ordering (11) has attracted attention to this family of compounds. The largest  $\gamma$  value of 850 mJ/mol K<sup>2</sup> was observed in  $U_2Pt_2In$ .

In order to investigate the effect of the variation of the number and characteristics of the  $5f$  electrons on the 2-2-1 compounds and further explore their stability limits it is important to study compounds based on available heavier actinides like Pu and Am. In this paper, the results of a systematic investigation of these 2-2-1 compounds with Pu and Am are reported.

## EXPERIMENTAL DETAILS

### Sample Preparation

To avoid excessive handling of the highly radioactive elements Pu and Am, attempts to synthesize  $Pu_2T_2X$  compounds were restricted to the  $T$  elements for which the isostructural U and Np compounds could be obtained, with

<sup>1</sup>To whom correspondence should be addressed.

$T = \text{Fe, Ru, Co, Rh, Ir, Ni, Pd, Pt}$  and  $X = \text{Sn, In}$ . With Am, only the compounds  $\text{Am}_2T_2\text{Sn}$  with  $T$  belonging to the Ni group were studied.

As already reported for the U and Np series (1, 3), the samples have been synthesized in glove boxes by arc melting stoichiometric amounts of the constituents under Ar atmosphere. In order to avoid oxidation due to slightly surface-oxidized plutonium and americium, those two metals were first remelted once individually. High-purity Pu and Am metals (99.7% and 99.5%, respectively) were obtained from commercially available oxides by a pyrometallurgical process and refined by evaporation in vacuum (12). Mass losses after arc-melting were less than 0.5%.

The single-phase character of the samples was checked both by metallography and by X-ray powder diffraction carried out on a Philips PW1120/90 generator with a Debye-Scherrer camera (114.6 mm diameter) using the  $\text{CuK}\beta$  radiation filtered out by Ni.

### Structure Determination

The X-ray structural analyses were performed using small single crystals obtained from crushed material; the lattice parameters, atomic positions, and atomic distances were determined by single-crystal X-ray diffraction on an En-

raf-Nonius four circle CAD-4 diffractometer with graphite-monochromated  $\text{MoK}\alpha$  radiation ( $\lambda = 0.71069 \text{ \AA}$ ) and  $\omega$ - $2\theta$  scan technique with the  $\Delta\omega = 0.90 + 0.35 \tan \theta$ . The lattice parameters were obtained by least-squares refinement of the setting angles of 17 to 25 reflections, according to the different compounds, using the Enraf-Nonius CAD-4 package. The intensities of three standard reflections were measured at 2 h intervals and anisotropic decay corrections were applied to the data. Absorption corrections were applied on the basis of  $\psi$  scan data obtained from 3 to 6 reflections according to the different compounds. The crystallographic calculations were made using the SDP program package (13). Details of the intensity data collection and crystallographic data for all the obtained 2-2-1 Pu and Am compounds are summarized in Tables 1 and 2.

### Physical Properties Measurements

The magnetic susceptibility of the  $\text{Pu}_2T_2X$  samples was measured, from room temperature to 1.8 K, using coarsely ground material and a transversal Faraday system with a custom-made helium cryostat. A resistive magnet (Brucker Analytische Messtechnik) with Henry-type pole caps provided fields up to 15000 Oe; the force was measured by a Sartorius type 4102 microbalance. Measurement and

TABLE 1  
Crystallographic Data for  $\text{Pu}_2T_2X$  and  $\text{Am}_2T_2\text{Sn}$  Intermetallic Compounds

Chemical formula	$\text{Pu}_2\text{Ni}_2\text{In}$	$\text{Pu}_2\text{Pd}_2\text{In}$	$\text{Pu}_2\text{Pt}_2\text{In}$	$\text{Pu}_2\text{Rh}_2\text{In}$	$\text{Pu}_2\text{Ni}_2\text{Sn}$	$\text{Pu}_2\text{Pd}_2\text{Sn}$	$\text{Pu}_2\text{Pt}_2\text{Sn}$	$\text{Am}_2\text{Ni}_2\text{Sn}$	$\text{Am}_2\text{Pd}_2\text{Sn}$
Formula weight (u.m.a.)	710.40	805.86	983.18	798.83	714.29	809.75	987.07	718.20	813.66
Space group	$P4/mbm$	$P4/mbm$	$P4/mbm$	$P4/mbm$	$P4/mbm$	$P4/mbm$	$P4/mbm$	$P4/mbm$	$P4/mbm$
Cell parameters									
Number of reflections and $\theta$ range for LS cell parameters	22 7.83–14.24	25 8.43–21.41	25 8.00–21.95	18 8.19–16.06	22 7.79–24.15	23 7.51–16.12	22 7.56–21.90	17 7.76–14.07	17 8.00–15.49
$a$ ( $\text{\AA}$ )	7.336(3)	7.657(2)	7.663(4)	7.451(3)	7.272(2)	7.607(2)	7.629(2)	7.315(3)	7.603(4)
$c$ ( $\text{\AA}$ )	3.690(2)	3.818(1)	3.795(1)	3.741(2)	3.745(1)	3.867(1)	3.806(1)	3.765(2)	3.851(3)
$V$ ( $\text{\AA}^3$ )	198.6(3)	223.8(2)	222.9(3)	207.7(3)	198.0(2)	223.7(2)	221.5(2)	201.4(3)	222.6(4)
$Z$	2	2	2	2	2	2	2	2	2
$\rho$ calculated ( $\text{g}\cdot\text{cm}^{-3}$ )	11.88	11.96	14.65	12.77	11.98	12.02	14.80	11.84	12.14
Crystal size ( $\times 10^{-2}$ mm <sup>3</sup> )	$8 \times 9 \times 14$	$2 \times 13 \times 20$	$6 \times 7 \times 31$	$4 \times 6 \times 15$	$6 \times 8 \times 30$	$4 \times 5 \times 21$	$3 \times 5 \times 23$	$6 \times 8 \times 33$	$3 \times 4 \times 27$
Data collected									
$\theta$ range	4.0–50.0	4.0–64.0	4.0–50.0	4.0–45.0	4.0–68.0	4.0–60.0	4.0–64.0	4.0–50.0	4.0–50.0
Range in $hkl$	$\pm 8, \pm 8, \pm 4$	$0+11, \pm 11, \pm 5$	$0-11, \pm 11, \pm 5$	$\pm 8, \pm 8, 0+4$	$\pm 11, \pm 11, 0+5$	$\pm 10, \pm 10, \pm 5$	$0+11, \pm 11, \pm 5$	$\pm 8, \pm 8, \pm 4$	$\pm 10, \pm 10, 0-5$
Number of reflections measured	1390	1670	1658	616	1805	2598	1641	1158	1467
Number of unique reflections	116	243	242	88	247	205	238	117	205
$R_{\text{int}}$ (on $F$ values)	0.070	0.031	0.072	0.051	0.031	0.049	0.049	0.048	0.056
Number of unique reflections with $I > 3\sigma(I)$	87	213	110	66	210	151	184	85	82
Decay corrections (min/max)	0.977/1.032	0.991/1.032	0.978/1.021	0.988/1.028	0.993/1.027	0.991/1.046	0.995/1.019	1.000/1.088	1.000/1.081
Number of reflections	4	6	4	4	6	5	5	6	3
$\theta$ range for $\Psi$ -scan									
absorption corrections	8.33–11.12	7.56–13.74	8.03–8.44	7.74–10.96	7.84–12.88	7.54–10.60	8.05–10.77	7.79–10.89	8.01–10.65
Transmission factors (min/max)	0.204/0.993	0.373/0.997	0.254/0.994	0.373/0.990	0.280/0.999	0.717/0.982	0.519/0.995	0.799/0.999	0.511/0.997
$\mu$ cm <sup>-1</sup>	539.26	473.21	1029.23	502.72	546.73	478.69	1040.80	—	—
$F_{000}$	586	658	786	654	588	660	788	592	664
$R^e$	0.045	0.043	0.066	0.070	0.029	0.055	0.073	0.048	0.048
$R_w^b$	0.066	0.072	0.080	0.098	0.048	0.080	0.096	0.086	0.065
Goodness-of-fit $S$	1.693	2.013	2.180	2.568	1.271	2.001	2.320	2.180	1.507
Secondary extinction coefficient	$1.85 \times 10^{-7}$	$2.15 \times 10^{-7}$	$3.10 \times 10^{-7}$	$5.50 \times 10^{-7}$	$3.50 \times 10^{-7}$	$2.40 \times 10^{-7}$	$2.20 \times 10^{-7}$	—	$2.40 \times 10^{-7}$
Number of variables	7	7	7	7	7	7	7	7	7

$$^a R = \sum [|F_o| - |F_c|] / \sum |F_o|$$

$$^b R_w = [\sum W [|F_o| - |F_c|]^2 / \sum W |F_o|^2]^{1/2}$$

**TABLE 2**  
**Atomic Positions and Interatomic Bonding Distances (pm) of  $\text{Pu}_2T_2X$  and  $\text{Am}_2T_2\text{Sn}$  Intermetallic Compounds**

Compound	$x_1$	$x_2$	$d_1(\text{An}-\text{An})$	$d_2(\text{An}-\text{An})$	$d_3(\text{An}-\text{An})$	$d(\text{An}-X)$	$d_1(\text{An}-T)$	$d_2(\text{An}-T)$	$d(T-X)$
$\text{Pu}_2\text{Ni}_2\text{Sn}$	0.1755	0.3773	374.5	360.9	379.4	372.2	279.6	289.0	288.5
$\text{Pu}_2\text{Pd}_2\text{Sn}$	0.1743	0.3707	386.7	373.7	397.4	341.1	286.3	303.2	298.9
$\text{Pu}_2\text{Pt}_2\text{Sn}$	0.1732	0.3705	380.6	373.7	399.1	340.3	285.6	301.0	299.5
$\text{Pu}_2\text{Ni}_2\text{In}$	0.1730	0.3747	369.0	358.9	383.8	328.2	279.0	288.3	289.8
$\text{Pu}_2\text{Pd}_2\text{In}$	0.1734	0.3713	381.8	375.6	400.4	341.5	287.0	301.8	300.9
$\text{Pu}_2\text{Pt}_2\text{In}$	0.1714	0.3702	379.5	371.6	401.7	341.6	287.1	300.5	300.6
$\text{Pu}_2\text{Rh}_2\text{In}$	0.1682	0.3638	374.1	354.5	392.0	334.4	278.4	295.0	289.5
$\text{Am}_2\text{Ni}_2\text{Sn}$	0.1743	0.3763	376.5	360.5	382.2	329.3	281.3	290.3	289.7
$\text{Am}_2\text{Pd}_2\text{Sn}$	0.1745	0.3713	385.1	375.4	397.1	340.5	286.0	302.4	298.8

regulation of the sample temperature was achieved by two independent Cu/constantan and Au-Fe/chromel thermocouples previously calibrated against a Pt and/or Ge resistor. This calibration was checked with three standard samples ( $\text{FeSO}_4 \cdot 7\text{H}_2\text{O}$ ,  $\text{CuSO}_4 \cdot 5\text{H}_2\text{O}$ , and  $\text{K}_2\text{Ni}(\text{SO}_4)_2 \cdot 6\text{H}_2\text{O}$ ) (14) to give an accuracy of  $\pm 0.02$  between 1.5 and 9.0 K. Susceptibility values were taken as the average of measurements at 9 different magnetic fields between 3000 and 15000 Oe. The field dependence observed was always very small ( $< 2\%$  at liquid  $\text{N}_2$  temperature) and for some compounds with a maximum of 7% at liquid He temperature. In all cases extrapolation to large fields gave values quite close to the average.

Electrical resistivity was measured using a standard four-probe ac method, in the 1.5–295 K temperature range using a lock-in technique. The resistivity samples were bar shaped cut directly from the arc-melted bulk material. The samples were mounted and encapsulated in a copper sample holder, sealed with “STYCAST” and decontaminated before being manipulated outside the glove box and placed inside an helium cryostat. The sample temperature was measured using a calibrated diode (Lake Shore DT-470) placed in close thermal contact with the sample holder.

## RESULTS AND DISCUSSION

### Structural Aspects

In Table 3 the compositions studied in this work are indicated together with those for which  $\text{An}_2T_2X$  compounds were previously reported. For  $\text{Pu}_2T_2\text{In}$  and  $\text{Pu}_2T_2\text{Sn}$  with  $T = \text{Ni}, \text{Pd},$  and  $\text{Pt}$ , the composition melted congruently and only the 2-2-1 phase was obtained, as indicated by metallographic examination and powder X-ray diffraction. In the case of  $\text{Pu}_2\text{Rh}_2\text{In}$  and  $\text{Am}_2T_2\text{Sn}$  with  $T = \text{Ni}$  and  $\text{Pd}$ , the compounds melted incongruently and the 2-2-1 phase was detected among other phases as  $\text{AnTX}$  and  $\text{An}_2T$ .

As indicated in Tables 1 and 2, single-crystal X-ray diffraction clearly indicates that the new  $\text{Pu}_2T_2X$  and


$\text{Am}_2T_2\text{Sn}$  compounds have the same tetragonal  $\text{U}_3\text{Si}_2$  structure type (space group  $P4/mbm$ ,  $Z = 2$ ) already described for the U and Np compounds (1, 3), with the An atom on  $4h$  ( $x_1, x_1 + 0.5, 0.5$ ),  $T$  on  $4g$  ( $x_2, x_2 + 0.5, 0$ ), and  $X$  on  $2a$  ( $0, 0, 0$ ) positions. The average values of  $x_1$  and  $x_2$  are, respectively, 0.17 and 0.37. A perspective view of this structure is shown in Fig. 1A. None of the Pu and Am compounds showed the superstructure reported for  $\text{U}_2\text{Pt}_2\text{Sn}$  and  $\text{U}_2\text{Ir}_2\text{Sn}$  (3).


Figure 1B shows the environment of an An atom. Besides the  $T$  and  $X$  atoms, each An atom has three types of An nearest neighbors; 2 neighbors along  $c$  at a distance which is the shortest  $d_1(\text{An}-\text{An})$  in almost all 2-2-1 U compounds and corresponds to the length of the  $c$  parameter, one neighbor within the basal plane at a distance which corresponds to the shortest  $d_2(\text{An}-\text{An})$  in most 2-2-1 Np, Pu, and Am compounds and finally, four neighbors, also in the basal plane, at a distance which corresponds to the largest  $d_3(\text{An}-\text{An})$  in the whole 2-2-1 family. The correspondent  $d(\text{An}-\text{An})$  values for these new Pu and Am compounds are also listed in Table 2. At least for the Pu compounds, these values are well above the Hill limit,  $\approx 3.4 \text{ \AA}$  for Pu (15). This means that there is a possibility that the An magnetic moments are not suppressed by the contribution of the 5f electrons due to the bonding as it is expected for the light actinides (up to Pu) which present an itinerant character (16).


The variation of the lattice parameters  $a$  and  $c$  with  $T$  substitution are shown in Figs. 2 and 3 for the isotypic Sn- and In-containing compounds with different An elements. The dependence of the unit-cell volume with An and  $T$  substitution is shown in Fig. 4 also for the same compounds. One can notice a significant increase of both  $a$  and  $c$  lattice parameters when a 3d element is replaced by the corresponding 4d element ( $\text{Co} \rightarrow \text{Rh}, \text{Ni} \rightarrow \text{Pd}$ ), certainly due to the noticeably greater metallic radii of the 4d elements. For the In compounds (Figs. 2a and 3a), with the substitution of a 5d element for a correspondent 4d element ( $\text{Rh} \rightarrow \text{Ir}, \text{Pd} \rightarrow \text{Pt}$ ), there is only a small increase of  $a$  but


TABLE 3  
Stability Domain of  $An_2T_2X$  Compounds

An	X	T							
		Fe	Ru	Co	Rh	Ir	Ni	Pd	Pt
U	In								
	ref. 1 Sn								
Np	In								
	refs. 1,3 Sn								
Pu	In								
	(*) Sn								
Am	In								
	(*) Sn								

 Light gray:  $An_2T_2X$  compounds with congruent melting and tetragonal structure  $U_3Si_2$  type,  $P4/mbm$ ,  $Z = 2$

 Dark gray:  $An_2T_2X$  compounds with congruent melting and tetragonal structure  $Zr_3Al_2$  type,  $P4_2/mnm$ ,  $Z = 4$

 Horizontal: Incongruent melting compounds where the  $An_2T_2X$  phase ( $U_3Si_2$  type structure) is present with  $AnTX$  and  $An_2T$ .

 Diagonal: Incongruent melting compounds with  $AnTX$  and  $An_2T$  phases and no detected traces of  $An_2T_2X$  phase.

(\*) This work.

a small decrease of  $c$ ; as the metallic radii in the  $4d$  and  $5d$  groups are similar, the changes in the unit cell volume (Fig. 4a) are not so significant.

Compared to the In compounds the  $c$  parameter is higher and, on the contrary, the  $a$  parameter is lower for all Sn compounds (Fig. 2a vs Fig. 2b and Fig. 3a vs Fig. 3b).

Concerning  $An$  substitutions, there is mostly a tendency to increase the  $c$  parameter (except for  $Np_2Pt_2In$ ,  $Np_2Ni_2Sn$ ,  $Am_2Pd_2Sn$ ), although the differences are not too significant. In contrast, the  $a$  parameter shows the opposite trend which results in only a slight increase of the volume. For different  $An$  elements, the unit-cell volume diagrams

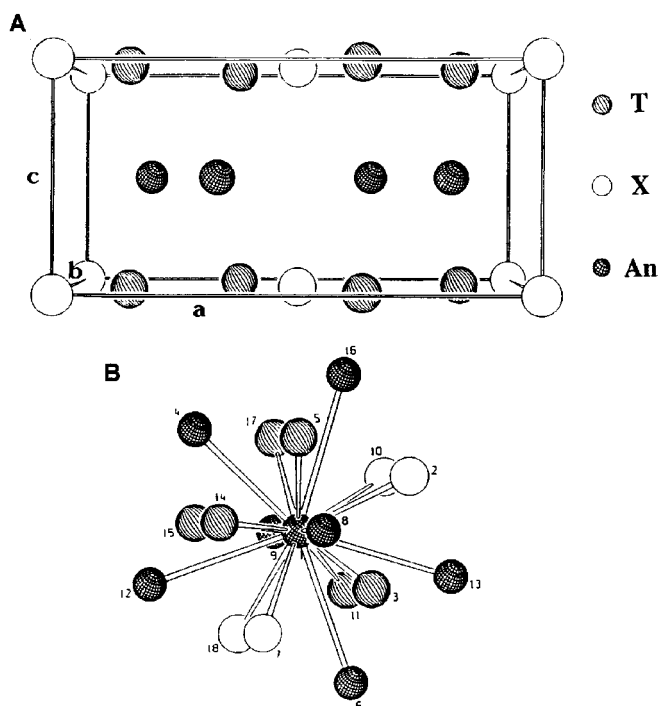


FIG. 1. (A) Structure of  $An_2T_2X$  in a perspective view; (B) environment of an Actinide atom in the tetragonal  $An_2T_2X$ .

(Fig. 4) show characteristic ranges of values for each type of 3d, 4d, and 5d groups of elements with almost no variation in both series for Sn and In compounds.

This behavior shows that the lattice parameters depend not only on steric effects, but also on the electronic structure of the different  $An$ ,  $T$ , and/or  $X$  (as In and Sn are in the same plane as  $T$ ) elements which interact with each other.

*Stability domain of the 2-2-1 family.* The decreasing number of 2-2-1 compounds obtained along the actinide series: 18 with U, 12 with Np, 7 with Pu, and 2 with Am (Table 1), suggests that the stability of this family decreases with the substitution of a heavier actinide element. However, this conclusion can be somewhat limited in the case of Am since only three compositions were tested with this actinide. Such behavior is probably due to the increasing localization degree of the actinide 5f states (16) and, since the highest stability is obtained for the Co and Ni groups, it can also reflect to electronic effects from the different transition metals. Indeed, for most of the U (2, 9, 17, 18) and Np (10) compounds studied up to now which contains a  $T$  element belonging to the Fe, Co, or Ni groups, magnetization results indicate that the 5f localization increases (i.e., the  $f-d$  hybridization decreases) with the filling of the  $d$  band: Fe < Co < Ni or Ru < Rh < Pd or Ir < Pt.

#### Magnetic Properties

The temperature dependence of the magnetic susceptibility,  $\chi(T)$ , of polycrystalline  $Pu_2T_2X$  samples ( $T = Ni, Pd, Pt$ ;  $X = Sn, In$ ) are shown in Fig. 5. The high-temperature data for all compounds can be fitted rather well to a modified Curie-Weiss law,  $\chi = \chi_0^* + C^*/(T - \Theta)$  with the

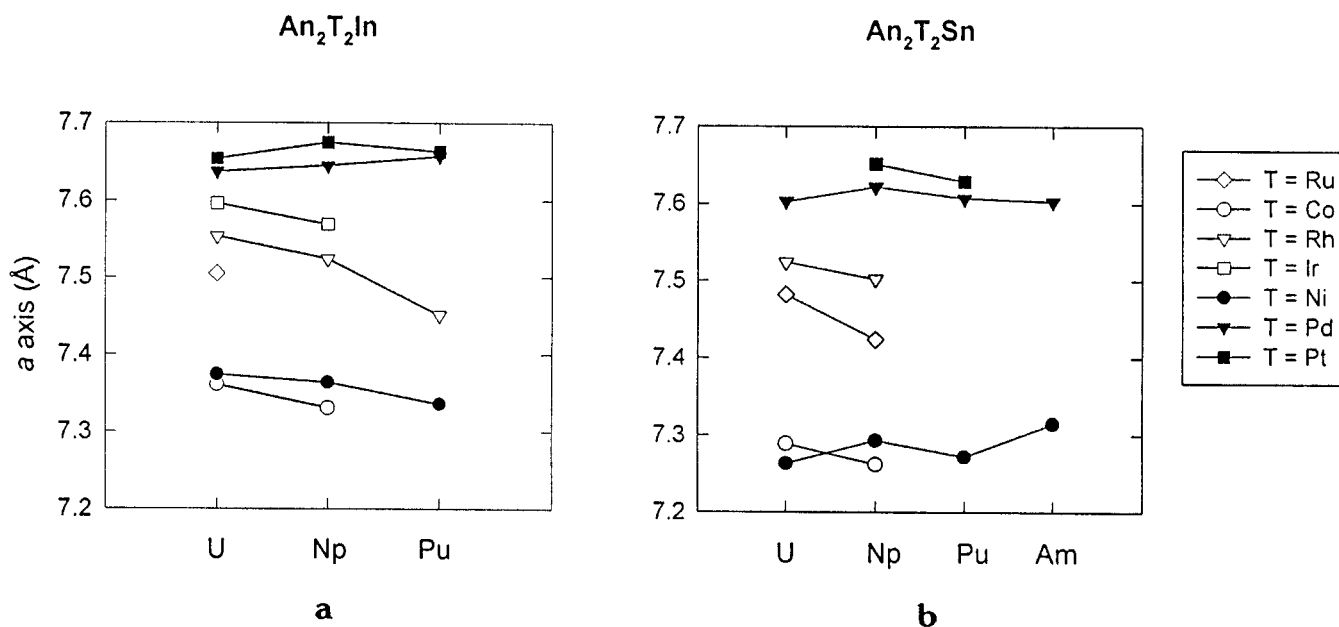


FIG. 2. Variation of the lattice parameter  $a$  (Å) for substitutions between isotopic (a) In- and (b) Sn-containing 2-2-1 compounds with different  $An$  and  $T$  elements.

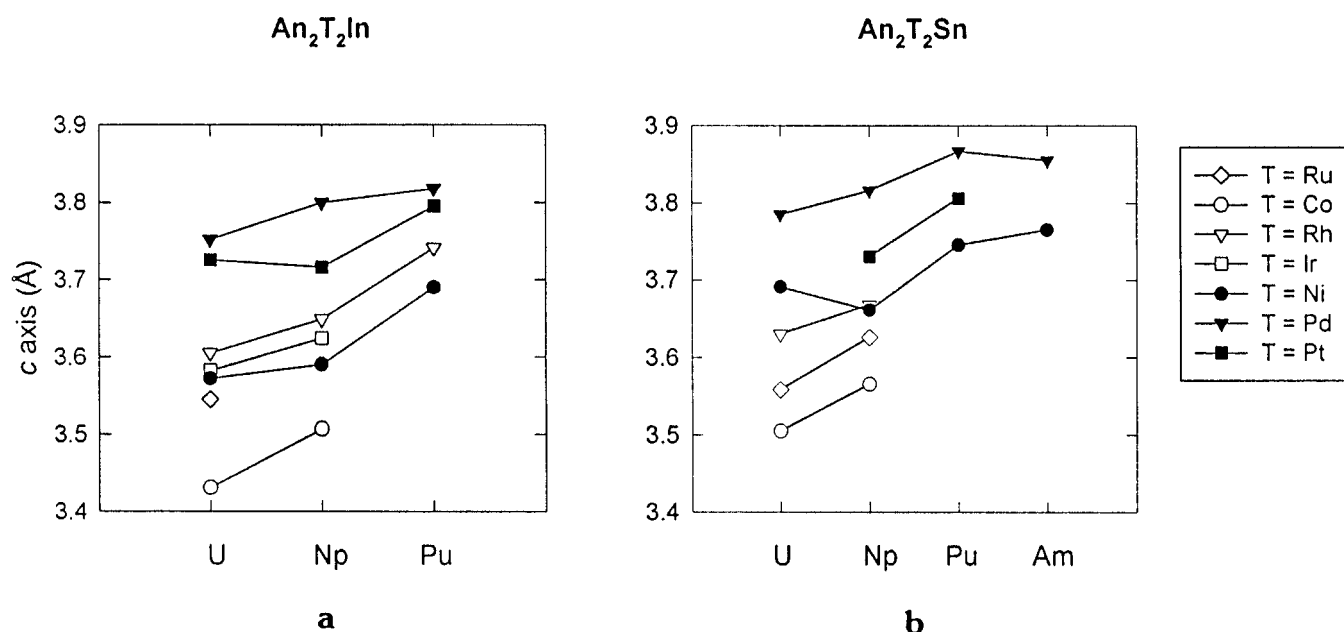


FIG. 3. Variation of the lattice parameter  $c$  (Å) for substitutions between isotypic (a) In- and (b) Sn- containing 2-2-1 compounds with different  $An$  and  $T$  elements.

parameters given in Table 4. This modified Curie–Weiss law indicates that, in addition to a possible small Pauli paramagnetic contribution, the susceptibility is dominated by a Van Vleck contribution due to groups of levels well separated in energy by crystal-field effects. The fitted  $\chi_0^*$  values in these compounds are quite similar to those previously found in analogue compounds with U (9). In all

compounds the  $\Theta$  values are negative, indicating the existence of antiferromagnetic interactions, although the values are consistently smaller in these Pu analogues than in the U analogues (9).

For a comparison of the different compounds and in order to extract physical quantities directly related to the crystal field ground state properties, renormalized  $\chi_0$  and

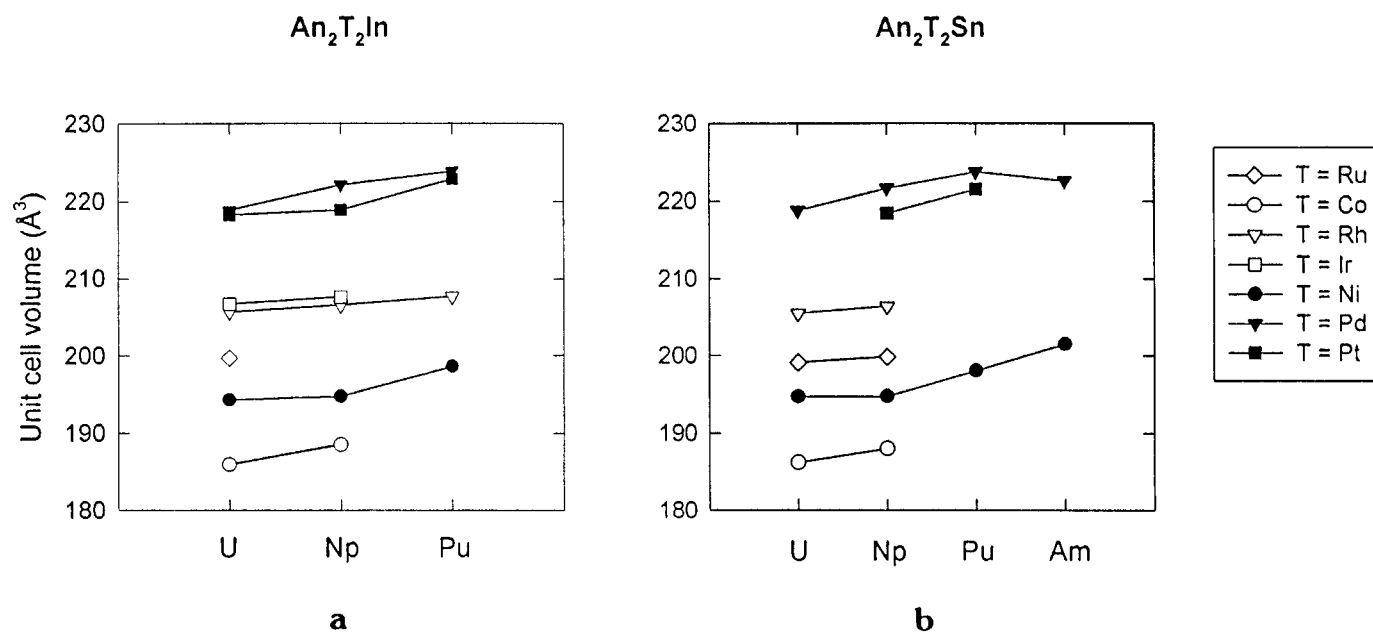


FIG. 4. Dependence of the unit-cell volume ( $\text{Å}^3$ ) with  $An$  and  $T$  elements for both (a) In and (b) Sn 2-2-1 compounds.

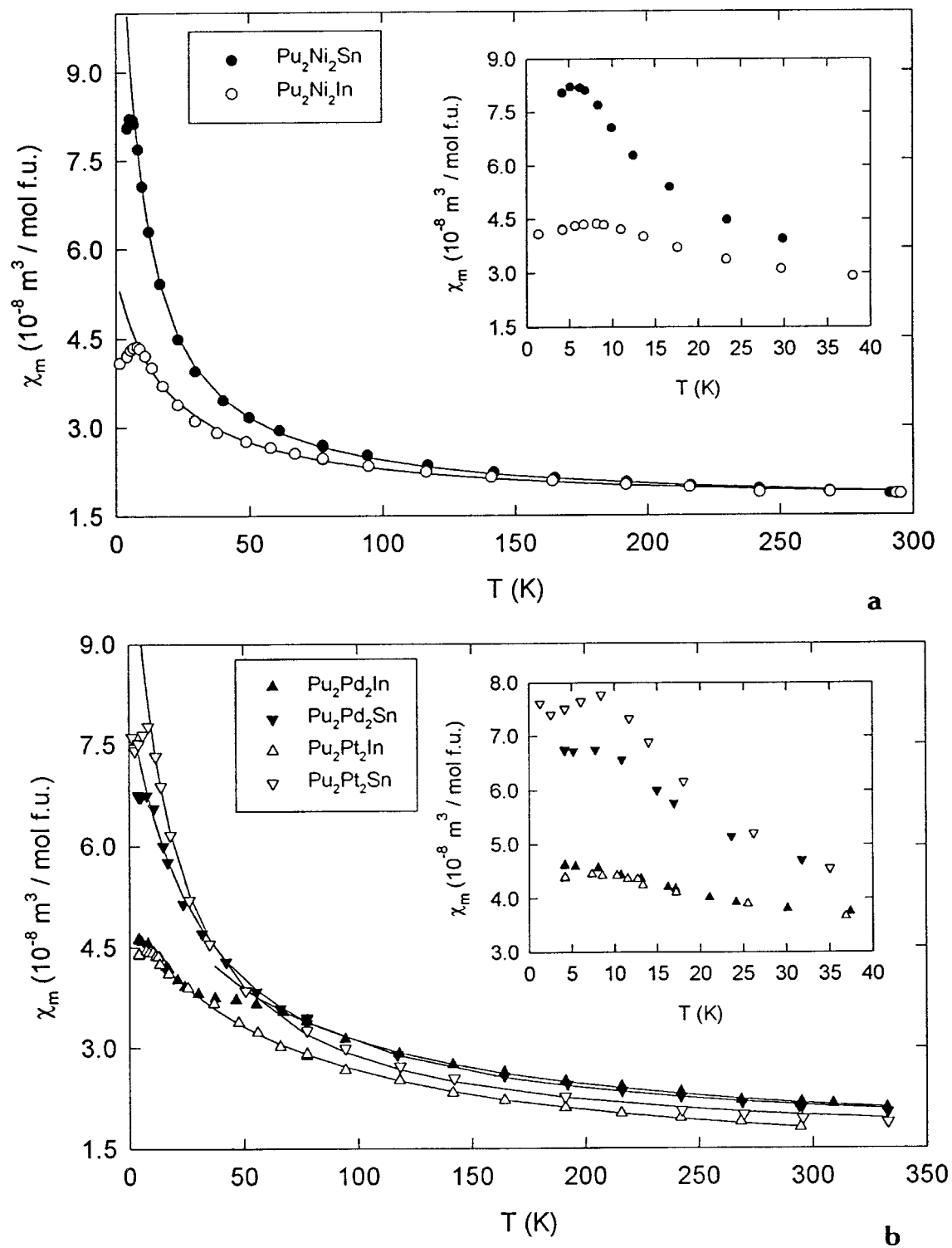


FIG. 5. Temperature dependence of the magnetic susceptibility of (a)  $\text{Pu}_2\text{Ni}_2X$  ( $X = \text{In, Sn}$ ) and (b)  $\text{Pu}_2T_2X$  ( $T = \text{Pd, Pt}; X = \text{In, Sn}$ ). The insets show in detail the low-temperature data. The solid lines are fits to the modified Curie-Weiss law (see text).

TABLE 4

Fitting Parameters of the Modified Curie–Weiss Law  $\chi = \chi_0^* + C^*/(T - \Theta)$  Applied to the Paramagnetic Susceptibilities and Corresponding Renormalized Parameters  $\chi_0$  and  $\mu_{\text{eff}}$  as Defined in Ref. (19)

Compound	$\chi_0^*(\times 10^{-8} \text{ m}^3/\text{mol})$	$\chi_0(\times 10^{-8} \text{ m}^3/\text{mol})$	$\Theta(\text{K})$	$\mu_{\text{eff}}^*(\mu_{\text{B}}/\text{Pu})$	$\mu_{\text{eff}}(\mu_{\text{B}}/\text{Pu})$
$\text{Pu}_2\text{Ni}_2\text{In}$	1.7	2.4	-19	0.35	0.50
$\text{Pu}_2\text{Pd}_2\text{In}$	1.4	1.8	-56	0.64	0.84
$\text{Pu}_2\text{Pt}_2\text{In}$	1.1	1.4	-72	0.67	0.86
$\text{Pu}_2\text{Ni}_2\text{Sn}$	1.6	1.8	-6	0.37	0.41
$\text{Pu}_2\text{Pd}_2\text{Sn}$	1.5	1.8	-30	0.56	0.69
$\text{Pu}_2\text{Pt}_2\text{Sn}$	1.5	1.7	-16	0.50	0.58

C constants, as defined by Amoretti and Fournier (19) are used instead (see Table 4). As expected for antiferromagnetic coupling we observe  $\chi_0 > \chi_0^*$  and  $C > C^*$ . For all these compounds the renormalized effective moments determined by the Curie constant  $C$  are substantially smaller compared with the full  $J$  of the  $5f^5$  configuration in the intermediate coupling scheme ( $\mu_{\text{eff}} = 1.01 \mu_{\text{B}}$  for  $\text{Pu}^{3+}$ ) (20). For both  $\text{Pu}_2\text{Pt}_2\text{In}$  and  $\text{Pu}_2\text{Pd}_2\text{In}$ , the renormalized effective moments are only slightly higher than the value expected for  $\text{Pu } 5f^5$ , corresponding to the crystal-field  $\Gamma_8$  configuration in the intermediate coupling scheme ( $\mu_{\text{eff}} = 0.80 \mu_{\text{B}}$  for  $\text{Pu}^{3+}$ ). For the remaining compounds, the effective magnetic moments are lower, approaching the  $\Gamma_7$  configuration value ( $\mu_{\text{eff}} = 0.49 \mu_{\text{B}}$ ) (20). The low renormalized effective moments denote the presence of large crystal-field interac-

tions in all of these compounds. It is also noticeable that  $\Theta$  values are more negative in Sn compounds than in the In compounds, indicative of stronger antiferromagnetic interactions.

With the exception of  $\text{Pu}_2\text{Ni}_2\text{In}$  and  $\text{Pu}_2\text{Pt}_2\text{Sn}$ , and in spite of the clear antiferromagnetic interactions, no clear indication of a magnetic transition is found at low temperatures. While in all other compounds the low-temperature data suggest a saturation or at most the existence of a broad maximum below  $\approx 6 \text{ K}$ , in these two compounds the maxima are much clearer and sharper, strongly suggesting an antiferromagnetic transition at 8 and 10 K, respectively. For  $\text{Pu}_2\text{Pd}_2\text{In}$  an anomaly is noticed at  $\approx 50 \text{ K}$ . The possibility of the presence of a magnetic impurity, responsible for this anomaly, cannot be entirely ruled out.

Without more detailed low-temperature data it is not possible to fully characterize the nature of the magnetic interaction in these compounds. However, it is clear that they are antiferromagnetic and of smaller magnitude than those observed for the U compounds, where U–U distances are generally below the Hill limit while here the Pu–Pu distances are higher than this limit.

### Electrical Properties

The temperature dependence of the electrical resistivity,  $\rho(T)$ , of polycrystalline  $\text{Pu}_2T_2\text{In}$  and  $\text{Pu}_2T_2\text{Sn}$  with  $T = \text{Ni, Pd, and Pt}$  is shown in Figs. 6 and 7, respectively.

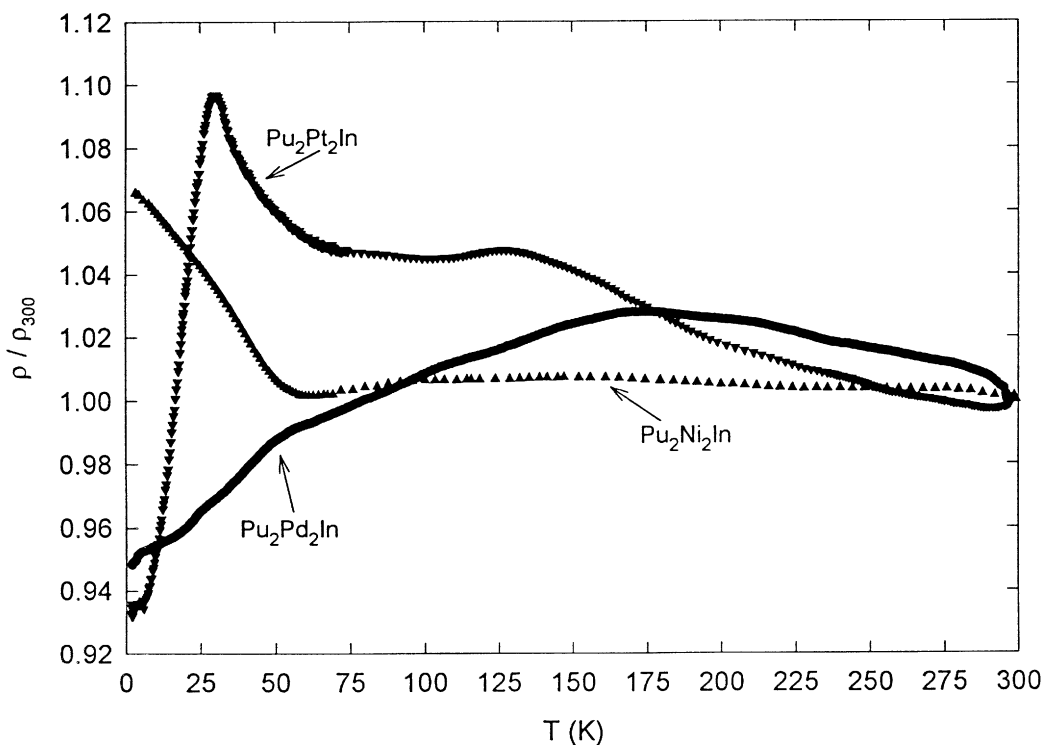


FIG. 6. Temperature dependence of the reduced electrical resistivity of  $\text{Pu}_2T_2\text{In}$  ( $T = \text{Ni, Pd, Pt}$ ).



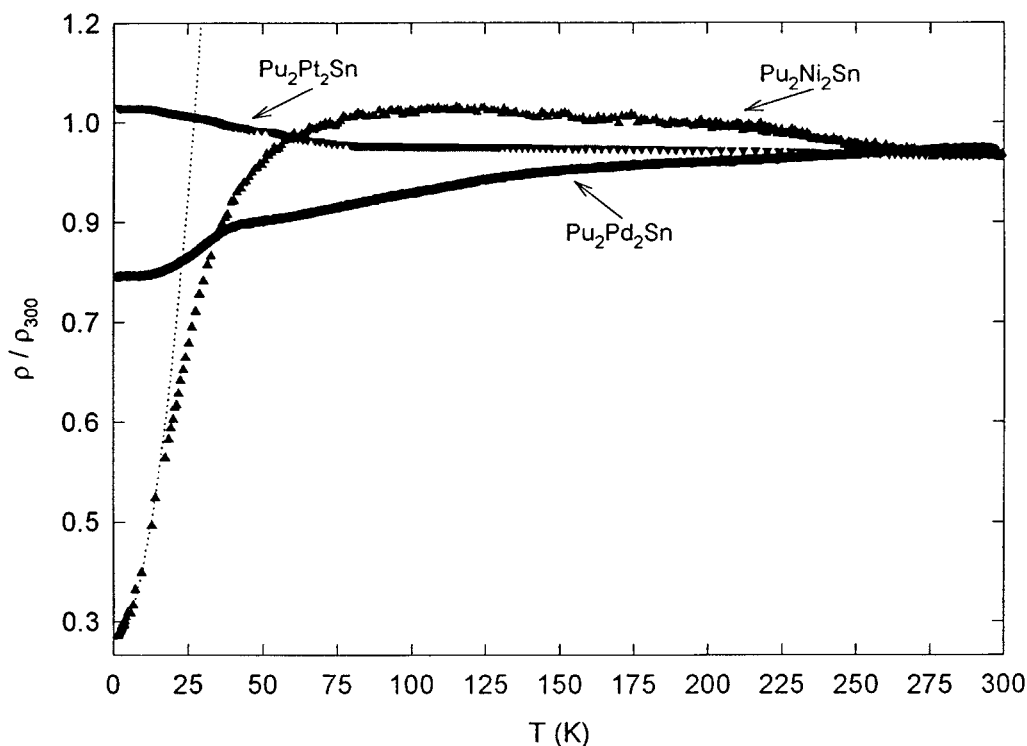


FIG. 7. Temperature dependence of the reduced electrical resistivity of  $\text{Pu}_2T_2\text{Sn}$  ( $T = \text{Ni, Pd, Pt}$ ). The dotted line is a fit of the low-temperature data ( $<9.5$  K) to a  $T^2$  law (see text).

The behavior of  $\text{Pu}_2\text{Pt}_2\text{In}$ , where the electrical resistivity has a plateau between 125 and 60 K, and then upon cooling reaches a very pronounced maximum in the vicinity of 30 K before it decreases rapidly down 1.4 K, is reminiscent of the behavior of some Pu intermetallics that were proved to be spin fluctuation systems (e.g.,  $\text{PuPtIn}$  (4) and  $\text{PuAl}_2$  (21)). The presence of this maximum around 30 K, a slightly higher temperature than that of the susceptibility maximum ( $\cong 10$  K), is similar to other systems described by spin fluctuation scattering effects (22); upon cooling below 30 K the sharp decrease of the electrical resistivity indicates that the random magnetic scatterers either disappear or become aligned.

For  $\text{Pu}_2\text{Ni}_2\text{Sn}$  a more typical spin fluctuating character, as in other heavy-fermion systems as  $\text{UPt}_3$ ,  $\text{CeCu}_2\text{Si}_2$ , and  $\text{UBe}_{13}$  (23), is observed. In this case the resistivity curve that remains constant at high temperatures starts to decrease significantly around 75 K, with no hint of magnetic ordering being observed down to 1.4 K. In this compound the resistivity  $\rho$  between 1.5 and 9.5 K follows a  $\rho = \rho_0 + AT^2$  law with  $A = 0.257 \mu\Omega\text{cm}/\text{K}^2$  and  $\rho_0 = 66.852 \mu\Omega\text{cm}$  (dotted line in Fig. 7), confirming a spin fluctuation behavior in narrow bands.

In  $\text{Pu}_2\text{Ni}_2\text{In}$  and  $\text{Pu}_2\text{Pt}_2\text{Sn}$ , a sudden increase of the electrical resistivity occurs below 60 and 80 K, respectively (Fig. 8). This type of resistivity increase is often associated with antiferromagnetic transitions. However, this is not the

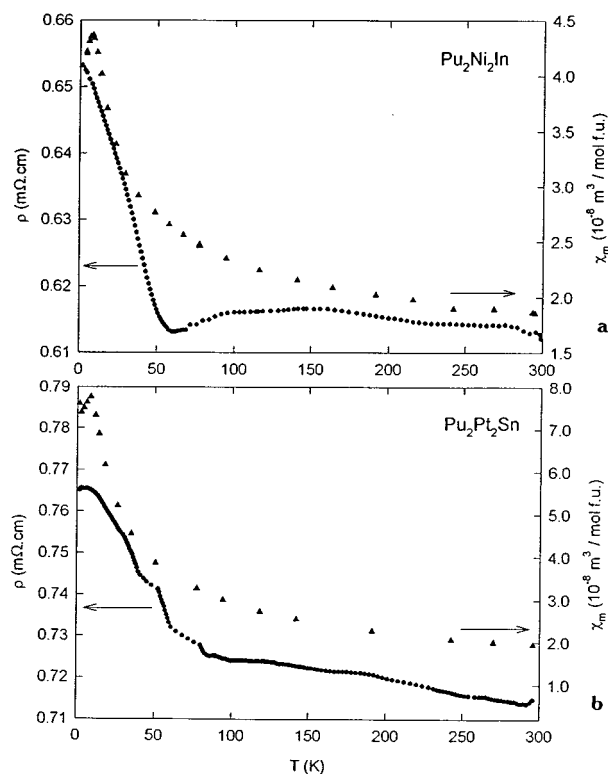


FIG. 8. Temperature dependence of the magnetic susceptibility and the electrical resistivity of (a)  $\text{Pu}_2\text{Ni}_2\text{In}$  and (b)  $\text{Pu}_2\text{Pt}_2\text{Sn}$ .

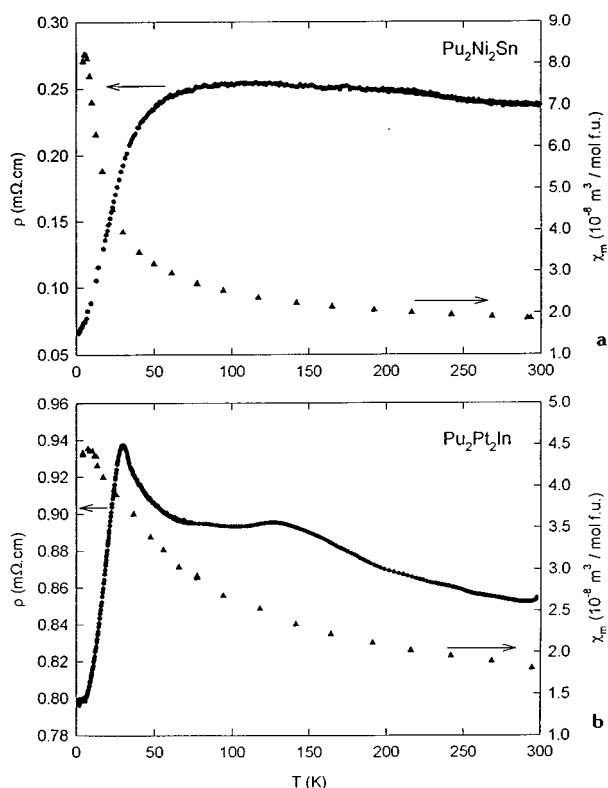


FIG. 9. Temperature dependence of the magnetic susceptibility and the electrical resistivity of (a)  $\text{Pu}_2\text{Ni}_2\text{Sn}$  and (b)  $\text{Pu}_2\text{Pt}_2\text{In}$ .

case in these compounds since the temperatures for which the anomalies in the resistivity curves occur are almost one order of magnitude higher than the susceptibility maxima (Figs. 8 and 9).

### CONCLUSIONS

Our trials to extend the number of 2-2-1 compounds using heavier actinide elements as Pu and Am allowed us to verify that this family remains isostructural, thereby preserving the tetragonal  $\text{U}_3\text{Si}_2$ -type structure in all studied compounds. However, it is also noticed that the number of compounds which stabilize the 2-2-1 phase decreases as the atomic number of the actinide element increases.

The magnitude of the magnetic interaction in the Pu compounds is smaller than those for U. An antiferromagnetic ground state is suggested only for  $\text{Pu}_2\text{Ni}_2\text{In}$  and  $\text{Pu}_2\text{Pt}_2\text{Sn}$  both by magnetic susceptibility and electrical resistivity data. Electrical resistivity at low temperatures in  $\text{Pu}_2\text{Pd}_2\text{Sn}$ ,  $\text{Pu}_2\text{Pt}_2\text{In}$ , and particularly in  $\text{Pu}_2\text{Ni}_2\text{Sn}$ , where a  $\rho = \rho_0 + AT^2$  law is observed, indicates the existence of spin fluctuation effects.

### ACKNOWLEDGMENTS

Support given to L. C. J. Pereira in the frame of the EC-funded training program "Human Capital and Mobility" and by PRAXIS

XXI program is acknowledged. The collaboration between Karlsruhe and Sacavém was supported by NATO Collaboration Research Grant 920996.

### REFERENCES

1. N. Péron, Y. Kergadallan, J. Rebizant, D. Meyer, J. M. Winand, S. Zwirner, L. Havela, H. Nakotte, J. C. Spirlet, G. M. Kalvius, E. Colineau, J. L. Oddou, C. Jeandey, and J. P. Sanchez, *J. Alloys Compd.* **201**, 203 (1993).
2. F. Mirambet, P. Gravereau, B. Chevalier, L. Trut, and J. Etourneau, *J. Alloys Compd.* **203**, 29 (1993).
3. L. C. J. Pereira, J. M. Winand, F. Wastin, J. Rebizant, and J. C. Spirlet, in "Proceedings, 24 ièmes Journées des Actinides", p. 109, Obergurgl, April 15–19, 1994.
4. V. Shechosvský and L. Havela, in "Ferromagnetic Materials" (E. P. Wohlfarth and K. H. J. Buschow, Eds.), Vol. 4, p. 309. North Holland, Amsterdam, 1988. [and references cited therein]
5. V. Shechosvský, L. Havela, H. Nakotte, F. R. de Boer, and E. Brück, *J. Alloys Compd.* **207/208**, 221 (1994).
6. H. Nakotte, K. Prokeš, E. Brück, N. Tang, F. R. de Boer, P. Svoboda, V. Shechosvský, L. Havela, J. M. Winand, A. Seret, J. Rebizant, and J. C. Spirlet, *Physica B* **201**, 247 (1994).
7. A. Purwanto, R. A. Robinson, L. Havela, V. Shechosvský, P. Svoboda, H. Nakotte, K. Prokeš, K. F. R. de Boer, A. Seret, J. M. Winand, J. Rebizant, and J. C. Spirlet, *Phys. Rev. B* **50**(10), 6792 (1994).
8. M. Diviš, M. Richter, and H. Eschrig, *Solid. State Comm.* **90**(2), 99 (1994).
9. L. Havela, V. Shechosvský, P. Svoboda, H. Nakotte, K. Prokeš, F. R. de Boer, A. Seret, J. M. Winand, J. Rebizant, J. C. Spirlet, A. Purwanto, and R. A. Robinson, *J. Magn. Magn. Mater.* **140–144**, 1367 (1995).
10. J. P. Sanchez, E. Colineau, C. Jeandey, J. L. Oddou, J. Rebizant, A. Seret, and J. C. Spirlet, *Physica B* **206** and **207**, 531 (1995).
11. L. Havela, V. Shechosvský, P. Svoboda, M. Diviš, H. Nakotte, K. Prokeš, F. R. de Boer, A. Purwanto, R. A. Robinson, A. Seret, J. M. Winand, J. Rebizant, J. C. Spirlet, M. Richter, and H. Eschrig, *J. Appl. Phys.* **76**(10), 6214 (1994).
12. J. C. Spirlet, *J. Nucl. Mater.* **166**, 41 (1989).
13. B. A. Frenz, Ver. SDPPlus V1.0, Enraf-Nonius, Delft (1986).
14. B. Kanellakopoulos, E. Heinrich, C. Keller, E. König, and F. Baumgärtner, *Chem. Phys.* **53**, 197 (1980).
15. H. H. Hill, in "Plutonium and Other Actinides 1970" (W. N. Miner, Ed.), AIME, New York, 1970.
16. M. S. S. Brooks, B. Johansson, and H. L. Skriver, in "Handbook on the Physics and Chemistry of Actinides" (A. J. Freeman and G. H. Lander, Eds.), Vol. 1, p. 153. North Holland, Amsterdam, 1984.
17. L. C. J. Pereira, A. Seret, F. Wastin, A. Hiess, J. P. Sanchez, J. Rebizant, and J. C. Spirlet, in "Proceedings, 25 ièmes Journées des Actinides," p. 124, L'Aquila, April 7–11, 1995.
18. K. Prokeš, E. Brück, H. Nakotte, P. F. de Châtel, and F. R. de Boer, *Physica B* **206** and **207**, 8 (1995).
19. G. Amoretti and J. M. Fournier, *J. Magn. Magn. Mater.* **43**, L217 (1984).
20. J. M. Fournier, in "Actinides—Chemistry and Physical Properties" (L. Manes, Ed.), Vol. 59/60, p. 127. Springer Verlag, Berlin, 1985.
21. A. J. Arko, M. B. Brodsky, and W. J. Nellis, *Bull. Amer. Phys. Soc.* **15**, 293 (1970).
22. S. H. Liu, in "Handbook on the Physics and Chemistry of Rare Earths" (K. A. Gshneidner, Jr., L. Eyring, G. H. Lander, and G. R. Choppin, Eds.), Vol. 17, p. 87. Elsevier, The Netherlands, 1993.
23. G. R. Stewart, *Rev. Mod. Phys.* **56**, 755 (1984).